International Journal of Nanomedicine

Dovepress
open access to scientific and medical research

Open Access Full Text Article

ORIGINAL RESEARCH

PEG-nanolized ultrasmall selenium nanoparticles overcome drug resistance in hepatocellular carcinoma HepG2 cells through induction of mitochondria dysfunction

Shanyuan Zheng[1,2]
Xiaoling Li[1]
Yibo Zhang[1]
Qiang Xie[3]
Yum-Shing Wong[2]
Wenjie Zheng[1]
Tianfeng Chen[1,3,4]

[1]Department of Chemistry, Jinan University, Guangzhou, China; [2]School of Life Sciences, The Chinese University of Hong Kong, Hong Kong, China; [3]Wu Jing Zong Dui Hospital of Guangdong Province, Guangzhou, China; [4]State Key Laboratory of Oncology in South China, Cancer Center, Sun Yat-sen University, Guangzhou, China

Correspondence: Tianfeng Chen
601 Huangpu Road,
Guangzhou 510632, China
Tel +86 20 8522 5962
Fax +86 20 8522 1263
Email felixchentf@gmail.com

Yum-Shing Wong
G92, School of Life Sciences,
The Chinese University of Hong Kong,
Hong Kong, China
Tel +852 2609 6389
Fax +852 2603 5745
Email yumshingwong@cuhk.edu.hk

Abstract: Gray selenium (Se) is one of the most widely used Se sources with very limited biocompatibility and bioactivity. In the present study, a simple method for the preparation of ultrasmall selenium nanoparticles (SeNPs) through direct nanolization of gray selenium by polyethylene glycol (PEG) was demonstrated. Monodisperse and homogeneous PEG-SeNPs with ultrasmall diameters were successfully prepared under optimized conditions. The products were characterized using various microscopic and spectroscopic methods, and the results suggest that the amphoteric properties of PEG and the coordination between oxygen and selenium atoms contributed to the formation of ultrasmall nanoparticles. PEG-SeNPs exhibited stronger growth inhibition on drug-resistant hepatocellular carcinoma (R-HepG2) cells than on normal HepG2 cells. Dose-dependent apoptosis was induced by PEG-SeNPs in R-HepG2 cells, as evidenced by an increase in the sub-G1 cell population. Further investigation on the underlying molecular mechanisms revealed that depletion of mitochondrial membrane potential and generation of superoxide anions contributed to PEG-SeNPs-induced apoptotic cell death in R-HepG2 cells. Our results suggest that PEG-SeNPs may be a candidate for further evaluation as a chemotherapeutic agent for drug-resistant liver cancer, and the strategy to use PEG200 as a surface decorator could be a highly efficient way to enhance the anticancer efficacy of nanomaterials.

Keywords: selenium, PEG, nanolization, drug resistance, apoptosis

Introduction

Cancer is a major challenge to public health, and among all cancer types, hepatocellular carcinoma is the fifth most common malignancy, affecting approximately one million people worldwide every year. It ranks third in cancer-related deaths, causing more than 600,000 deaths annually around the world.[1] The affected hepatocellular carcinoma population is mainly in Asia and Africa. However, recent reports have revealed an increasing incidence of primary liver cancer in the United States and Europe.[2] Such an increase is likely to continue for several decades, making hepatocellular carcinoma a more threatening disease to human beings. Doxorubicin-based combination chemotherapy is the main treatment for hepatocellular carcinoma, but its efficacy is limited due to the drug resistance of cancer cells.[3] To date, there is still no effective treatment for intermediate and end-stage hepatocellular carcinoma. Therefore, anticancer agents that can overcome drug resistance and enhance hepatoma cell death in advanced liver cancer are urgently needed.

submit your manuscript | www.dovepress.com
Dovepress
http://dx.doi.org/10.2147/IJN.S30940

Recently, the combination of biotechnology and nanotechnology has led to the development of cancer nanotechnology, manifested in broad applications in molecular imaging, molecular diagnosis, and targeted therapy, providing new hope in cancer treatments.[4,5] The basic rationale is that nanoscaled materials have structural, optical, or magnetic properties that are not available from the molecules or bulk solids.[6] Selenium (Se) is a mineral trace element of fundamental importance to humans and animals. The role of Se as potential cancer chemotherapeutic and chemopreventive agents has been supported by many epidemiological, preclinical, and clinical studies.[7,8] Se nanoparticles (SeNPs) have attracted increasing attention in the past decade because of their antioxidant activities and low toxicity.[9,10] Compared to other nanoparticles that are currently most often studied, such as gold nanoparticles, SeNPs are superior, because Se is degradable in vivo. Degraded Se can be used as a nutrient for many kinds of normal cells or as an antiproliferative agent for many kinds of cancer cells.[11] Gold nanoparticles only act as carriers or tools for drugs and display no biological activities themselves, while SeNPs, by nature, display desired biological activities and can be drug carriers as well.

Polyethylene glycol (PEG) is the most widely used biocompatible polymer for chemical and biological applications.[12] It is the most popular polymer for protein conjugation,[13] and it has been used to functionalize proteins and peptides for drug delivery.[14,15] PEGylation has become a leading approach for overcoming most of the limits of the therapeutic application of new proteins, such as rapid body clearance, immunogenicity, physical and chemical instabilities (eg, aggregation, adsorption, deamination, clipping, oxidation), and enzymatic degradation.[16] PEG has a role in reducing the rapid kidney clearance of a given protein by increasing its hydrodynamic volume, reducing protein aggregation by repulsion between PEGylated surfaces. PEG also has a role in preventing immunogenicity and increasing the thermal stability of proteins. The toxicology profile of PEG is very safe, with evidence of side effects only at very high doses.[16,17] PEG is also known to be safe – it is FDA approved for use in injectable, topical, rectal, and nasal formulations.[13] With such favorable characteristics, PEGylation has achieved great versatility in the protein modification field after years of research. However, while PEG exhibits great advantages in protein modification, using PEG as a carrier or modifying agent for bioactive molecules is still under exploration, and few research studies have reported using PEG for Se nanolization, especially for direct nanolization.

To date, most of the methods used to prepare SeNPs have used redox reaction and have involved many complex procedures. The introduction of reducers and the complex redox reaction create various side-products, which require much time and effort for purification, thus greatly limiting further investigation and practical use of SeNPs. Gray Se is one of the most widely used Se sources, with very limited biocompatibility. Turning crystalloid gray Se directly into atomic or atom-clustered Se by heating and dispersing in liquid phase, without the need for any redox reaction, is a much more convenient, environmentally friendly, and promising method of preparing SeNPs. Except for the biocompatibilities mentioned previously, PEG is able to remain stable when heated to high temperatures. Thus, in the present work, it is of interest to prepare PEG-nanolized Se-NPs (PEG-SeNPs) by dispersing gray Se in heated PEG. This system is prepared under high temperatures (215°C–220°C); as such, the nanoparticles should be able to undergo sterilization, which is a common difficulty of nanoparticles. The in vitro anticancer activity of PEG-SeNPs against drug-resistant hepatocellular carcinoma (R-HepG2) cells and the possible action mechanisms were also examined. Our results show that the as-prepared ultrasmall PEG-SeNPs were able to overcome drug resistance in R-HepG2 cells through the induction of mitochondria dysfunction.

Materials and methods

Materials

Thiazolyl blue tetrazolium bromide (MTT), propidium iodide (PI), solid JC-1, dihydroethidium diacetate, and doxorubicin (DOX) were purchased from Sigma-Aldrich Co (St Louis, MO). LysoTracker® Red was purchased from Molecular Probes (Carlsbad, CA). Gray selenium powder was purchased from Guangzhou Dinggang Chemical Factory (Guangzhou, China). PEG200 was purchased from Guangdong Chemical Technology Research Center (Guangzhou, China). The water used for all experiments was ultrapure, supplied by a Milli-Q water purification system from Millipore (Billerica, MA). All of the solvents used were of high-performance liquid chromatography (HPLC) grade.

Preparation and characterization of PEG-SeNPs

PEG-SeNPs were prepared by dissolving 40 mg gray Se powder in 10 mL PEG200 solution at 210°C–220°C for 15–20 minutes, under magnetic stirring. The product was then mixed with water in a 1:1 ratio. The solution was centrifuged at 10,000 rpm for 10 minutes and then washed with Milli-Q water five times to remove excess PEG. The obtained products were characterized by various spectroscopic and microscopic methods. Transmission electron microscope (TEM) samples

were prepared by dispersing the samples onto a holey carbon film on copper grids. The micrographs were obtained on a Hitachi H-7650 TEM (Hitachi Ltd, Tokyo, Japan) operated at an accelerating voltage of 80 kV. Scanning electron microscope energy-dispersive X-ray spectroscopy (SEM–EDX) analysis was carried out on an EX-250 system (HORIBA Ltd, Kyoto, Japan) and employed to examine the elemental composition.[18,19] Fourier transform infrared (FTIR) spectra of the samples were recorded on an EQVINOX 55 FTIR spectrometer (Spectrum™ One; PerkinElmer Inc, Waltham, MA), in the 400–4000 cm^{-1} range. To determine the in vitro cellular uptake of PEG-SeNPs, nanoparticles containing fluorescent dye 6-coumarin were prepared using a similar procedure, except that coumarin-6 (0.1 mg/mL) was added to the reaction system after the gray Se powder was totally dissolved into the PEG. The incorporated dye acted as a probe for PSP–SeNPs and offered a sensitive method to determine their intracellular uptake and localization.

Cell culture

Human hepatoma cell line (HepG2) was purchased from American Type Culture Collection (ATCC, Manassas, VA). The cell line was cultured in RPMI 1640 medium (Gibco®; Life Technologies Corporation, Carlsbad, CA) supplemented with 10% (v/v) fetal bovine serum (FBS) (Life Technologies) and 1% (v/v) penicillin–streptomycin (PS, 10,000 U/mL; Life Technologies) in a humidified atmosphere of 5% CO_2 in air, at 37°C. To develop a drug-resistant human hepatoma cell line (R-HepG2), HepG2 cells were cultured in the presence of DOX. The survival cells were treated stepwise with a higher concentration of DOX from 0.1 to 100 μM during cell passages. After more than ten selection rounds, a clone of R-HepG2 cells with DOX drug resistance was obtained. To maintain the drug resistance, the R-HepG2 cells were cultured and maintained in medium containing 1.2 μM DOX. From time to time, the sensitivity of the cells to DOX and other anti-cancer agents was analyzed to confirm their resistance to DOX.[3] The obtained R-HepG2 cells were about 50-, 3.3-, and 2.5-fold more resistant to DOX, cisplatin, and taxol, respectively, when compared to the corresponding IC_{50} values of the parental HepG2 cells,[20] indicating that the R-HepG2 cells exhibited drug resistance to a variety of functionally and structurally unrelated chemotherapeutic agents.

In vitro cellular uptake and localization of PEG–SeNPs

The intracellular localization of coumarin-6-loaded PEG-SeNPs in the R-HepG2 cells was traced with the lysosomal marker LysoTracker® Red. Briefly, the cells were cultured on cover glass in 6-well plates until 70% confluence was reached. Then, 80 nM LysoTracker was added and incubated for about 30 minutes. The cells, thus pretreated, were then incubated with 20 μg/mL 6-coumarin-loaded PEG-SeNPs for various periods of time. The cells were then washed three times using phosphate buffered saline (PBS) and examined under a fluorescence microscope (Nikon Eclipse 80i; NIKON CORPORATION, Tokyo, Japan).

Cell viability assay

Cell viability was determined by measuring the ability of the cells to metabolize thiazolyl bluse tetrazolium bromide (MTT) to a purple formazan dye.[21] Briefly, the cells were placed into 96-well plates at a density of 2.0×10^3 cells/well. After 24 hours, different concentrations of PEG-SeNPs were added and incubated for 72 hours. Then, 20 μL/well of MTT solution (5 mg/mL in PBS buffer) was added and incubated for another 5 hours. The medium was removed and replaced with 150 μL/well of dimethyl sulfoxide to dissolve the formazan crystals. Absorbance at 570 nm was taken on a 96-well microplate reader.

Flow cytometric analysis

DNA flow cytometric analysis was carried out according to our previously described method.[21] Briefly, cells exposed to PEG-SeNPs were harvested by centrifugation and washed with PBS. The cells were stained with PI (1.21 mg/mL Tris, 700 U/mL RNase, 50.1 mg/mL PI, pH 8.0) after fixing with 70% ethanol at −20°C overnight. DNA content was analyzed on a Beckman Coulter Epics XL MCL flow cytometer (Beckman Coulter, Inc, Miami, FL). Cell cycle distribution was analyzed using MultiCycle software (Phoenix Flow Systems, San Diego, CA). The proportion of cells in G0/G1, S, and G2/M phases were represented as a DNA histogram. Apoptotic cells with hypodiploid DNA content were measured by quantifying the sub-G1 peak in the cell cycle pattern. For each experiment, 10,000 events per sample were recorded.

Terminal deoxynucleotidyl transferase dUTP nick end labeling (TUNEL) assay and 4′,6-diamidino-2-phenylindole (DAPI) staining

The cells, cultured in chamber slides, were fixed with 3.7% formaldehyde for 10 minutes and permeabilized with 0.1% Triton X-100 in PBS. After that, the cells were incubated with 100 μL/well TUNEL reaction mixture (containing nucleotide

mixture and terminal deoxynucleotidyl transferase) for 1 hour and 1 g/mL of DAPI for 15 minutes, at 37°C. The cells were then washed with PBS and examined under a fluorescence microscope (Nikon Eclipse 80i).

Measurement of intracellular superoxide anion generation

Dihydroethidium (DHE) is a fluorogenic probe, highly selective for superoxide anion (O_2^-) among reactive oxygen species (ROS), which is freely permeable to cells and is oxidized by superoxide to ethidium bromide with red fluorescence; thus, the fluorescence intensity parallels the level of intracellular superoxide anion.[22] The treated cells were harvested and loaded with DHE at a final concentration of 10 μM, at 37°C for 25 minutes. The cells were then washed twice with PBS and suspended in PBS. The intracellular fluorescence was measured by flow cytometry.

Evaluation of mitochondrial membrane potential (ΔΨm)

The cells, cultured in 6-well plates, were trypsinized and resuspended in 0.5 mL of PBS buffer containing 10 μg/mL JC-1. After incubation for 10 minutes at 37°C, the cells were immediately centrifuged to remove the supernatant, and the cell pellets were suspended in PBS and then analyzed by flow cytometry. The percentage of green fluorescence from the JC-1 monomers was used to represent the cells that lost ΔΨm.

Statistical analysis

The experiments were carried out at least in triplicate, and the results were expressed as mean ± SD. Statistical analysis was performed using SPSS statistical package (SPSS 13.0 for Windows; IBM Corporation, Armonk, NY). Differences between two groups were analyzed by two-tailed Student's *t*-tests, and differences between three or more groups were analyzed by one-way analysis of variance (ANOVA) multiple comparisons. Differences with $P < 0.05$ (*) or $P < 0.01$ (**) were considered statistically significant.

Results and discussion

Preparation and characterization of PEG-SeNPs

In this study, ultrasmall PEG-SeNPs were successfully prepared under optimized conditions and characterized by various spectroscopic and microscopic methods. TEM images showed that the PEG-SeNPs presented monodisperse and homogeneous spherical structures with an average diameter of about 5 nm (Figure 1A). A size distribution histogram shows an average diameter of 28.7 ± 4.2 nm (Figure 1B), indicating that the PEG-SeNPs had Se cores about 5 nm in diameter, and the coated PEG gave them coronas and hydrodynamic diameters of about 28.7 nm. A surface elemental composition analysis of the PEG-SeNPs using SEM–EDX showed a strong Se atom signal (73.1%), along with C (24.2%) and O (2.7%) atom signals, from PEG (Figure 1C). No obvious peaks for other elements or impurities were observed in the spectrum. These results confirm the conjugation of PEG to the surface of the Se-NPs. FTIR analysis was conducted to characterize the changes in chemical bonds that occurred during the formation of the PEG-SeNPs. Figure 2 shows the FTIR spectra of gray Se powders, PEG200, and PEG-SeNPs. The FTIR PEG-SeNP spectrum resembles that of PEG, providing clear evidence that PEG forms part of the nanocomposite. The PEG200 spectrum showed characteristic bands of specific functional groups,

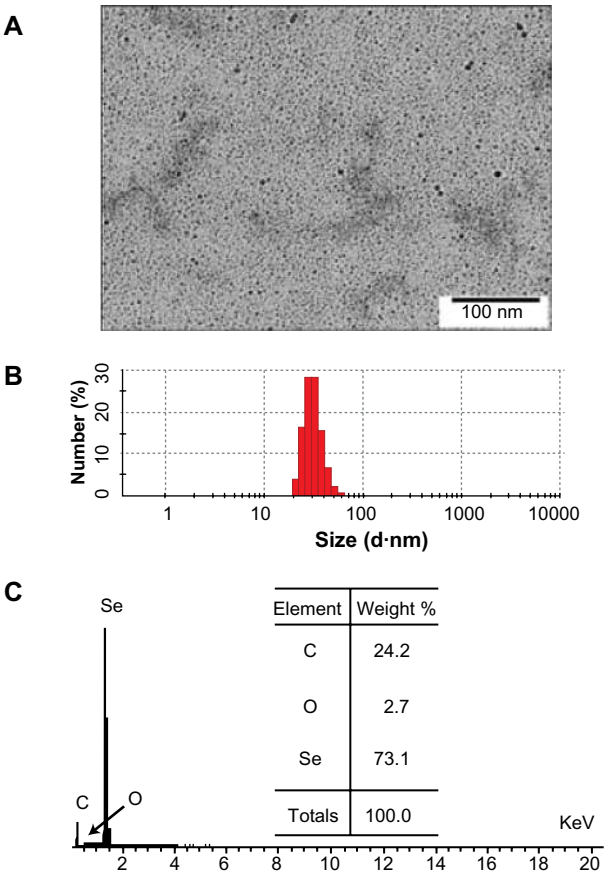

Figure 1 (**A**) TEM images, (**B**) size distribution, and (**C**) SEM-EDX analysis of PEG-SeNPs.

Abbreviations: Se, selenium; TEM, transmission electron microscopy; SEM-EDX, scanning electron microscope energy-dispersive X-ray spectroscopy; PEG-SeNPs, polyethylene-glycol-nanolized selenium nanoparticles.

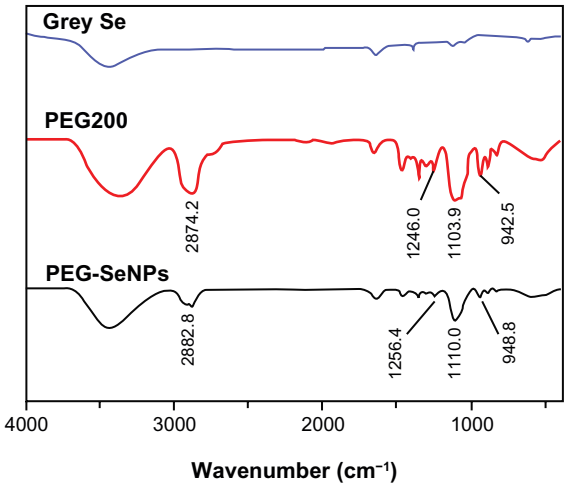

Figure 2 FTIR spectra of PEG-SeNPs.
Abbreviations: Se, Selenium; PEG-SeNPs, polyethylene-glycol-nanolized selenium nanoparticles; FTIR, Fourier transform infrared.

such as the bands appearing at 2874.2 cm^{-1} assigned to the –CH group[23] and the band at 1103.9 cm^{-1} assigned to the –C–O–C group.[24] These two characteristic bands and some other bands near 1103.9 cm^{-1} also appeared in the PEG-SeNP spectrum, indicating the successful conjugation of PEG to the surface of the SeNPs. Moreover, the peaks at 2874.2 and 1103.9 cm^{-1} shifted to 2882.8 and 1110.0 cm^{-1}, respectively, suggesting the occurrence of coordination between oxygen atoms in the –C–O–C group and the Se atom. Details about the structure of the PEG-SeNPs will be discussed in the schematic model.

In vitro cellular uptake and localization of PEG-SeNPs

Endocytosis is one of the most important uptake mechanisms for extracellular materials, especially nanomaterials. In this study, in order to track PEG-SeNPs during cellular uptake in cancer cells, we loaded PEG-SeNPs with 6-coumarin as a fluorescence probe. The intracellular localization of PEG-SeNPs in R-HepG2 cells were investigated by applying a specific probe, LysoTracker Red, for the fluorescence imaging of lysosomes. As shown in Figure 3, PEG-SeNPs were uptaken by the cells and located in lysosomes after a 1-hour treatment. The combination of the green and red fluorescence clearly indicated the co-localization of PEG-SeNPs and lysosomes in R-HepG2 cells. As time increased, some PEG-SeNPs escaped from lysosomes and

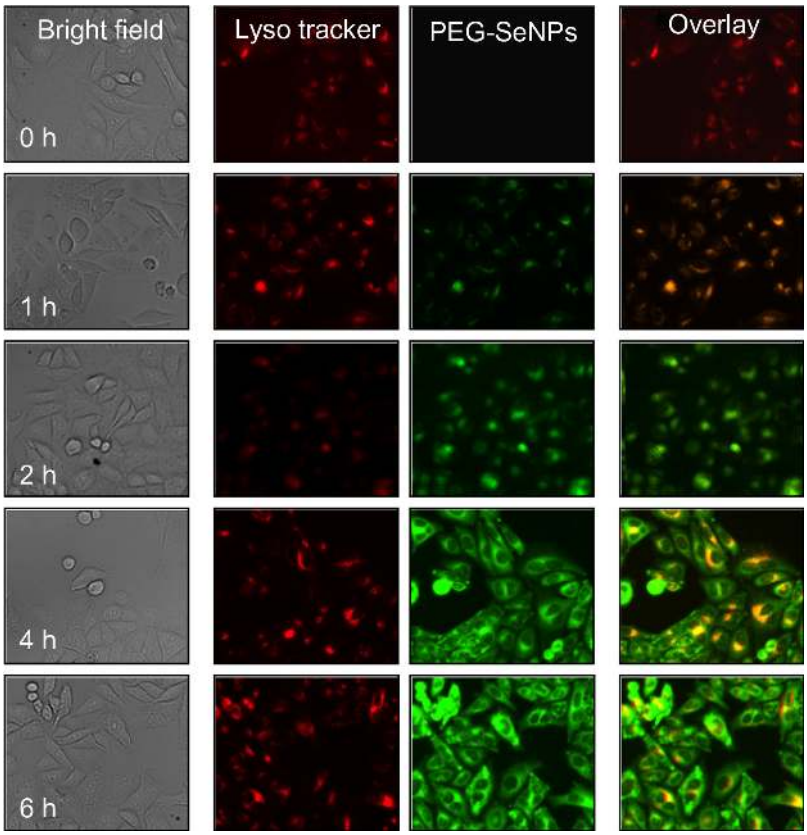

Figure 3 Cellular uptake and intracellular localization of 6-coumarin-loaded PEG-SeNPs in R-HepG2 cells.
Abbreviations: PEG-SeNPs, polyethylene-glycol-nanolized selenium nanoparticles; R-HepG2, drug-resistant hepatocellular carcinoma.

diffused into cytoplasm. At 6 hours, green fluorescence of 6-coumarin-loaded PEG-SeNPs could be observed in the entire cells. These results indicate that endocytosis is the major mechanism for the cellular uptake of PEG-SeNPs in cancer cells.

In vitro anticancer activity of PEG-SeNPs

The in vitro anticancer activity of PEG-SeNPs against HepG2 and R-HepG2 cell lines was evaluated by means of MTT assay. The results (Figure 4A) show that the PEG-SeNPs exhibited dose-dependent growth inhibition on both HepG2 and R-HepG2 cells. The inhibitory effects of the PEG-SeNPs were significantly higher on the R-HepG2 cells than on the HepG2 cells. For instance, the PEG-SeNPs at 2, 4, 8, and 16 μg/mL reduced R-HepG2 cell viability to 75.2%, 34.97%, 17.76%, and 14.8%, respectively. All of those values were significantly lower than those of the HepG2 cells (83.7%, 85.4%, 51.7% and 24.1%, respectively). Based on the chemical composition of the PEG-SeNPs obtained by EDX analysis, we compared the cytotoxicity of the SeNPs and PEG, separately, against the susceptible R-HepG2 cells at corresponding concentrations to examine their contribution to the anticancer action of the PEG-SeNPs. As shown in Figure 4B, the SeNPs alone, at concentrations of 8 and 12 μg/mL, slightly decreased cell viability to 94.8% and 88.9%, respectively, of the control group, whereas PEG200 at 1, 2, and 4 μg/mL reduced cell viability to 83.5%, 81.2%, and 76.2%, respectively. These results clearly demonstrate the synergetic effects of PEG on SeNPs through surface decoration. Interestingly, we found that a mixture of PEG200 and SeNPs displayed a much lower cytotoxic effect on R-HepG2 cells (IC50 value: 38.2 μg/mL) than did PEG-SeNPs (IC50 value: 3.27 μg/mL). Moreover, morphological observation after MTT staining showed that R-HepG2 cells treated with PEG-SeNPs exhibited a dose-dependent reduction in cell numbers, loss of cell-to-cell contact, cell shrinkage, and formation of apoptotic bodies (Figure 4C). Despite this potency, PEG-SeNPs showed much lower cytotoxicity toward normal cells (human kidney HK-2 cells) (Figure 4A). These results suggest that PEG-SeNPs possess great selectivity between cancer and normal cells. As the balance between therapeutic potential and toxic side effects of a compound is very important when evaluating its usefulness as a pharmacological drug, our results suggest that PEG-SeNPs display application potential in chemotherapy of drug-resistant liver cancer.

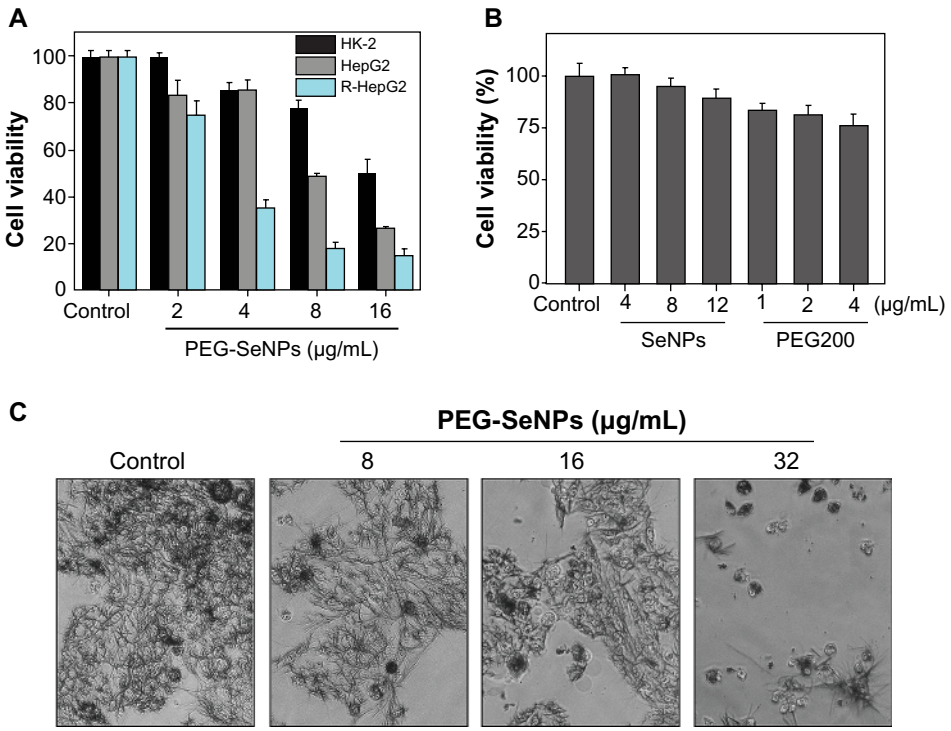

Figure 4 In vitro anticancer activity of PEG-SeNPs. (**A**) R-HepG2 and HepG2 cells were treated with PEG-SeNPs for 72 hours, and cell viability was determined by MTT assay. (**B**) R-HepG2 cells were treated with indicated concentrations of SeNPs or PEG200 alone for 72 hours, and cell viability was determined by MTT assay. (**C**) Morphology of R-HepG2 cells treated with PEG-SeNPs for 72 hours and stained by MTT (magnification, 200×).

Abbreviations: PEG-SeNPs, polyethylene-glycol-nanolized selenium nanoparticles; R-HepG2, drug-resistant hepatocellular carcinoma; HepG2, hepatocellular carcinoma; MTT, thiazolyl blue tetrazolium bromide.

PEG-SeNPs inhibit R-HepG2 cell growth though induction of apoptosis

Inhibition of proliferation in cancer cells treated with anticancer drugs could be the result of induction of apoptosis, cell cycle arrest, or a combination of these two modes.[3] Many studies have supported that apoptosis is one of the most essential mechanisms in cancer chemoprevention and chemotherapy by Se compounds.[8,25,26] In order to delineate the action modes of PEG-SeNPs in R-HepG2 cells, in vitro DNA detection assay-flow cytometry was carried out in this study. Figure 5 shows the representative DNA distribution histograms of R-HepG2 cells exposed to different concentrations of PEG-SeNPs. The results revealed that a dose-dependent increase in the percentage of cells in sub-G1 phase was observed in cells treated with 0.5–4.0 μg/mL PEG-SeNPs. For instance, the sub-G1 cell population increased from 7.7% (control) to 23.3% (4 μg/mL). However, no significant changes in G0/G1, S, or G2/M phases were observed in treated cells, suggesting that cell death induced by PEG-SeNPs was caused mainly by cell apoptosis. In contrast, in HepG-2 cells exposed to concentrations of PEG-SeNPs (0–4 μg/mL), no significant increase in sub-G1 peak was detected, suggesting that lower apoptotic cell death was induced in HepG-2 cells by PEG-SeNPs (Figure 5). The induction of apoptosis in R-HepG2 cells was further confirmed by DNA fragmentation and nuclear condensation as detected by TUNEL–DAPI co-staining assay. DNA fragmentation is an important biochemical hallmark of cell apoptosis. TUNEL assay can be used to detect the early stage of DNA fragmentation in apoptotic cells prior to changes in cell morphology. As shown in Figure 6, dose-dependent increases in DNA fragmentation and nuclear condensation were observed in R-HepG2 cells exposed to 4 and 8 μg/mL of PEG-SeNPs for 48 hours. Taken together, our results suggest that apoptosis is the major mode of cell death induced by PEG-SeNPs in drug-resistant liver cancer cells.

PEG-SeNPs induces cell apoptosis via mitochondrial dysfunction

Apoptosis is characterized by cell shrinkage, cytoplasmic and nuclear condensation, membrane blebbing, DNA fragmentation, and, finally, the formation of apoptotic bodies, followed by secondary necrosis. Apoptosis plays an essential role in the development of multicellular organisms.[27] Nowadays, the roles of apoptosis in the action of anticancer drugs have become increasingly clearer.[28] Mitochondria act as a point of integration for apoptotic signals originating from both the extrinsic and intrinsic pathways. Disruption of ΔΨm and release of apoptogenic factors are critical events in both caspase-dependent and -independent apoptotic pathways.[29] Thus, the status of ΔΨm was investigated in PEG-SeNP-treated R-HepG2 cells by JC-1 flow cytometric analysis. As shown in Figure 7, the PEG-SeNPs induced a dose-dependent increase in the depletion of ΔΨm in R-HepG2 cells, as evidenced by the shift of fluorescence from red to green. For instance, the percentage of cells with depolarized mitochondria increased from 13.4% (control) to 52.6% (4 μg/mL). These results indicate that mitochondria dysfunction contributes to PEG-SeNPs-induced apoptotic cell death. In contrast, in HepG-2 cells exposed to concentrations of PEG-SeNPs (0–4 μg/mL),

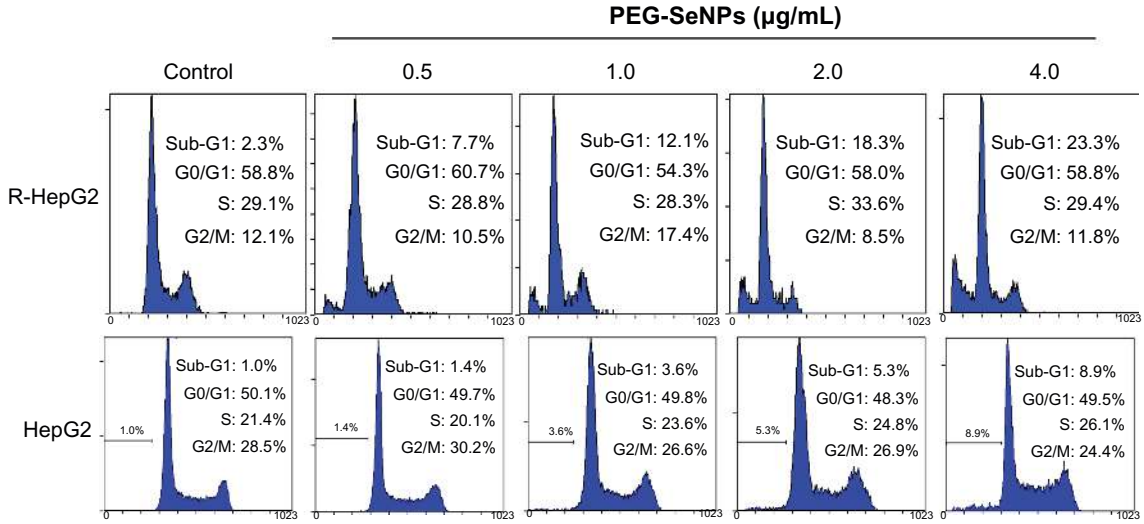

Figure 5 Flow cytometric analysis of cell cycle distribution of R-HepG2 cells treated with PEG-SeNPs for 72 hours.
Abbreviations: PEG-SeNPs, polyethylene-glycol-nanolized selenium nanoparticles; R-HepG2, drug-resistant hepatocellular carcinoma; HepG2, hepatocellular carcinoma.

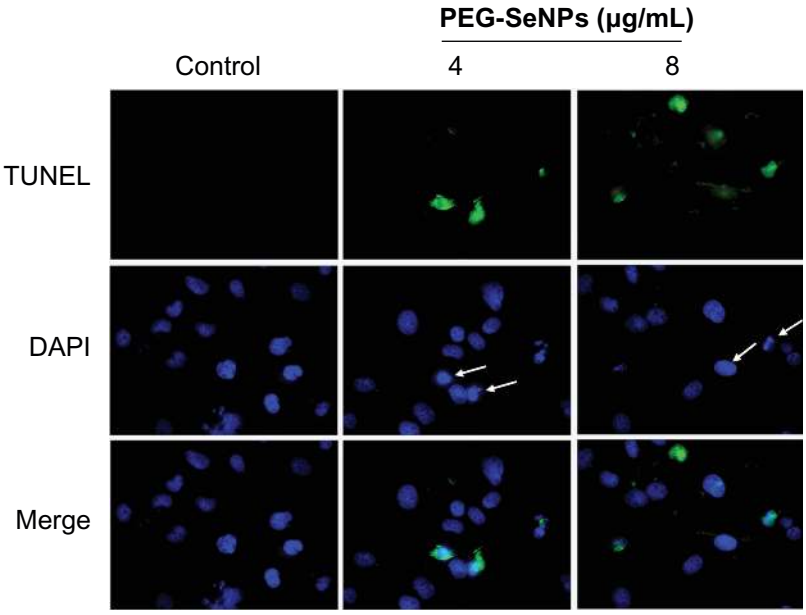

Figure 6 Representative photomicrographs of DNA fragmentation and nuclear condensation in response to PEG-SeNP treatment, as detected by TUNEL assay and DAPI staining. R-HepG2 cells were treated with 4 and 8 μg/mL PEG-SeNPs for 48 hours.
Abbreviations: PEG-SeNPs, polyethylene-glycol-nanolized selenium nanoparticles; TUNEL, terminal deoxynucleotidyl transferase dUTP nick end labeling; DAPI, 4′,6-diamidino-2-phenylindole; R-HepG2, drug-resistant hepatocellular carcinoma.

a much lower depletion rate of ΔΨm was found. For instance, the percentage of cells with depolarized mitochondria increased from 1.9% (control) to 22.3% (4 μg/mL), which was significantly lower than in R-HepG2 cells (Figure 7).

Reactive oxygen species (ROS) are highly reactive molecules that include free radicals, oxygen ions, and peroxides. ROS are constantly generated and eliminated in all biological systems. They are generated as a natural byproduct of normal cellular metabolism and have important roles in cell signaling. The mitochondrial respiratory chain is a potential source of ROS, and reduced mitochondria membrane potential leads to increased generation of ROS in apoptosis.[30] On the other hand, oxidative damage to the mitochondrial membrane due to increased generation of ROS has been reported to play a role in apoptosis.[31] Growing evidence suggests that ROS acts as a critical mediator in cell apoptosis, and that its generation is an important cellular event induced by Se compounds, resulting in cell apoptosis.[32] Thus, the intracellular level of superoxide anion, a major ROS, was determined by using the fluorescence dye DHE, a compound oxidized to the fluorescent DNA intercalating agent ethidium in proportion to the amount of superoxide present. The results showed that treatments of PEG-SeNPs led to dose- and time-dependent increases in intracellular superoxide anion level (Figure 8A). In contrast, in HepG-2 cells exposed to concentrations of PEG-SeNPs (2 and 4 μg/mL), much lower superoxide anion

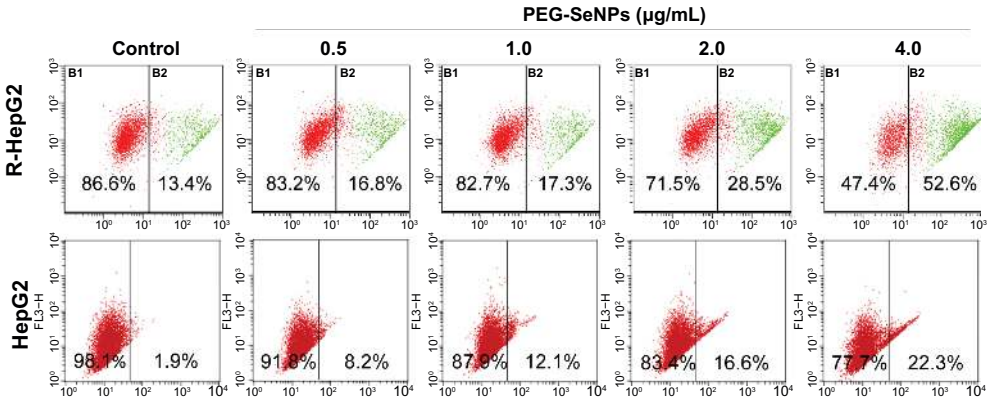

Figure 7 Loss of mitochondrial membrane potential in R-HepG2 cells treated with PEG-SeNPs for 72 hours.
Abbreviations: PEG-SeNPs, polyethylene-glycol-nanolized selenium nanoparticles; R-HepG2, drug-resistant hepatocellular carcinoma; HepG2, hepatocellular carcinoma.

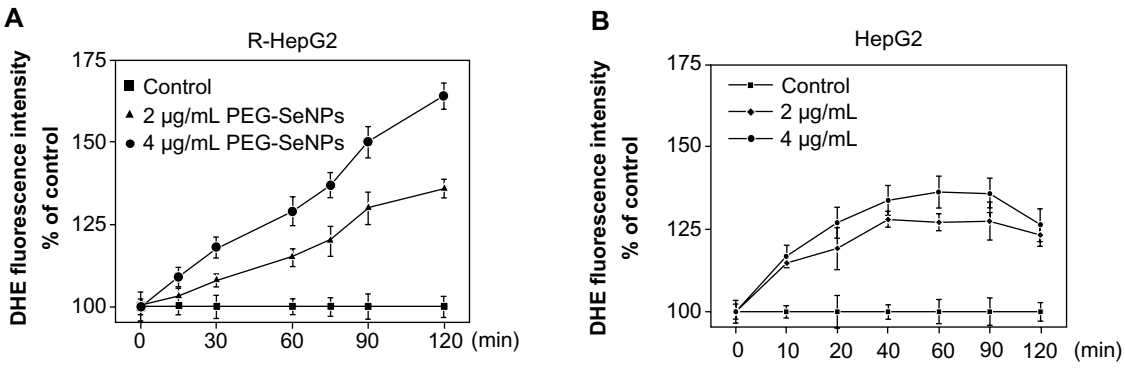

Figure 8 (**A** and **B**) Induction of superoxide anion generation in R-HepG2 and HepG2 cells by PEG-SeNPs.
Abbreviations: R-HepG2, drug-resistant hepatocellular carcinoma; DHE, dihydroethidium; HepG2, hepatocellular carcinoma; PEG-SeNPs, polyethylene-glycol-nanolized selenium nanoparticles.

production was found (Figure 8B). These results demonstrate the important role of superoxide anions in PEG-SeNPs-induced mitochondria dysfunction and cell apoptosis.

Schematic model of PEG-SeNPs

Research studies have indicated that the size of nanoparticles plays an important role in their biological activities; generally, smaller nanoparticles are more active than are larger ones.[33] More recent studies have suggested that nanoparticles appear to be a useful approach to overcoming drug resistance, because nanoparticles have the potential to bypass P-glycoprotein to evade efflux as they enter cells via endocytosis.[34] In addition, micelles decorated with PEG and PEG derivants might inhibit P-glycoprotein function to reverse drug resistance via interaction with cell membranes to affect the membrane microenvironment.[34] Thus, the ability of PEG-SeNPs to overcome drug resistance might be due to their PEG decoration and their ultrasmall diameters. In an effort to obtain a better understanding in the future of the mechanism by which PEG-SeNPs overcome drug resistance, we propose a schematic model for the preparation of PEG-SeNPs (Figure 9).

In the PEG chain, the oxygen atom is sp^3 hybridized, thus forming two carbon–oxygen covalent bonds and two lone-pair electrons. When gray Se powders dissolve in PEG solution, Se is in the form of clusters that consist of sp^3 hybridized Se atoms.

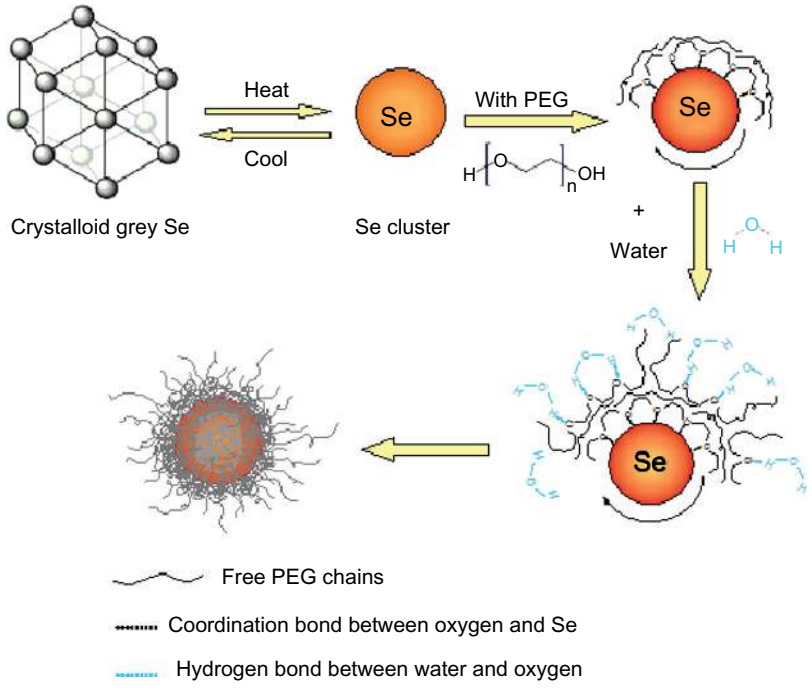

Figure 9 Schematic illustration of the preparation of PEG-SeNP.
Abbreviations: Se, selenium; PEG, polyethylene glycol; PEG-SeNP, polyethylene-glycol-nanolized selenium nanoparticle.

Each Se atom within offers empty 4d orbitals for coordination with lone-pair oxygen electrons. In this way, PEG chains assemble on the surface of SeNPs. Here, PEG effectively facilitates and accelerates the atomic clusterization of gray Se. Furthermore, it controls and retains the ultrasmall diameter of PEG-SeNPs in room temperature. Without the presence of PEG, the Se clusters would easily aggregate and turn back to gray Se when the temperature is cooled down. When this solution was mixed with water, the oxygen atoms, which are the hydrophilic parts of the PEG chain, turned forward due to a strong coordination with water molecules like hydrogen bonds.[16] Thus, the PEG-SeNPs are well dispersed in the aqueous solution. The cluster size of Se in the solution contributes to the ultrasmall diameters of the PEG-SeNPs.

In this system, PEG not only acts as a decoration agent to nanolize gray Se and a capping agent to prevent the aggregation of ultrasmall nanoparticles, but it also might help to overcome drug resistance. Furthermore, it is very likely to play a role in achieving combination and synergism of SeNPs with other anticancer drugs or bioactive molecules in the future. The use of PEG in the functionalization of nanomaterials has a bright future in cancer treatments. The polymer conjugation of anticancer drugs is very likely to achieve the following advantages: (1) elevated tumor accumulation due to the enhanced permeability and retention effect; and (2) selectivity of cancer cells through specific targeting by combining antibodies or other molecules recognized by the cancer cells. Based on this model, it is possible to wrap drugs, targeting molecules, or both inside PEG-SeNPs or to link targeting molecules to the terminal of coating PEG to achieve possible synergetic effects, cancer cell selectivity, or even both. The integrated drugs prepared thusly have a huge potential to exhibit multi-functional activities. In addition, such drugs are likely to possess favorable characteristics in vivo, due to their potential controlled release capacity. It has already been proven that the addition of PEG to lipidic implants is a very efficient tool for adjusting desired protein release patterns.[35] Moreover, research studies have indicated that a PEG coating around the nanocarrier helps to improve its stability in the biological fluids and facilitates the transport of bioactive molecules across the intestinal and nasal epithelia,[36,37] thereby offering great hope of developing an oral drug delivery system. Thus, the PEG-SeNPs system described in this paper is likely to be an efficient method for drug integration design in the future.

Conclusion

In the present study, a simple method for the preparation of ultrasmall SeNPs through direct nanolization of gray selenium by PEG was demonstrated. Monodisperse and homogeneous PEG-SeNPs with ultrasmall diameters were successfully prepared under optimized conditions. The ultrasmall PEG-SeNPs were able to overcome drug resistance in hepatocellular carcinoma cells, through induction of mitochondria dysfunction. Our results suggest that PEG-SeNPs may be a candidate for further evaluation as a chemotherapeutic agent for drug-resistant liver cancer, and the strategy of using PEG200 as a surface decorator could be a highly efficient way of enhancing the anticancer efficacy of nanomaterials.

Acknowledgments

This work was supported by National Science and Technology support program (2012BAC07B05), Natural Science Foundation of China and Guangdong Province, the Fundamental Research Funds for the Central Universities, Program for New Century Excellent Talents in University, and CUHK-IPMBAB Research Grant.

Disclosure

The authors report no conflicts of interest in this work.

References

1. Bosch FX, Ribes J, Diaz M, Cleries R. Primary liver cancer: worldwide incidence and trends. *Gastroenterology*. 2004;127(5 Suppl 1):S5–S16.
2. El-Serag HB. Hepatocellular carcinoma: recent trends in the United States. *Gastroenterology*. 2004;127(5 Suppl 1):S27–S34.
3. Ong RC, Lei J, Lee RK, et al. Polyphyllin D induces mitochondrial fragmentation and acts directly on the mitochondria to induce apoptosis in drug-resistant HepG2 cells. *Cancer Lett*. 2008;261(2):158–164.
4. Nie S, Xing Y, Kim GJ, Simons JW. Nanotechnology applications in cancer. *Annu Rev Biomed Eng*. 2007;9:257–288.
5. Zheng JS, Zheng SY, Zhang YB, et al. Sialic acid surface decoration enhances cellular uptake and apoptosis-inducing activity of selenium nanoparticles. *Colloids Surf B Biointerfaces*. 2011;83(1):183–187.
6. Sahoo SK, Parveen S, Panda JJ. The present and future of nanotechnology in human health care. *Nanomedicine*. 2007;3(1):20–31.
7. Nel A, Xia T, Madler L, Li N. Toxic potential of materials at the nanolevel. *Science*. 2006;311(5761):622–627.
8. Sinha R, El-Bayoumy K. Apoptosis is a critical cellular event in cancer chemoprevention and chemotherapy by selenium compounds. *Curr Cancer Drug Targets*. 2004;4(1):13–28.
9. Wang H, Zhang J, Yu H. Elemental selenium at nano size possesses lower toxicity without compromising the fundamental effect on selenoenzymes: comparison with selenomethionine in mice. *Free Radic Biol Med*. 2007;42(10):1524–1533.
10. Zhang J, Wang X, Xu T. Elemental selenium at nano size (Nano-Se) as a potential chemopreventive agent with reduced risk of selenium toxicity: comparison with se-methylselenocysteine in mice. *Toxicol Sci*. 2008;101(1):22–31.
11. Tran PA, Sarin L, Hurt RH, Webster TJ. Differential effects of nano-selenium doping on healthy and cancerous osteoblasts in coculture on titanium. *Int J Nanomedicine*. 2010;5:351–358.
12. Kohler N, Fryxell GE, Zhang M. A bifunctional poly(ethylene glycol) silane immobilized on metallic oxide-based nanoparticles for conjugation with cell targeting agents. *J Am Chem Soc*. 2004;126(23):7206–7211.

13. Treetharnmathurot B, Ovartlarnporn C, Wungsintaweekul J, Duncan R, Wiwattanapatapee R. Effect of PEG molecular weight and linking chemistry on the biological activity and thermal stability of PEGylated trypsin. *Int J Pharm*. 2008;357(1–2):252–259.
14. Aronov O, Horowitz AT, Gabizon A, Gibson D. Folate-targeted PEG as a potential carrier for carboplatin analogs. Synthesis and in vitro studies. *Bioconjug Chem*. 2003;14(3):563–574.
15. Roberts MJ, Bentley MD, Harris JM. Chemistry for peptide and protein PEGylation. *Adv Drug Deliv Rev*. 2002;54(4):459–476.
16. Pasut G, Veronese FM. State of the art in PEGylation: The great versatility achieved after forty years of research. *J Control Release*. November 7, 2011. [Epub ahead of print.]
17. Fruijtier-Polloth C. Safety assessment on polyethylene glycols (PEGs) and their derivatives as used in cosmetic products. *Toxicology*. 2005;214(1–2):1–38.
18. Deng Z, Cao L, Tang F, Zou B. A new route to zinc-blende CdSe nanocrystals: mechanism and synthesis. *J Phys Chem B*. 2005;109(35):16671–16675.
19. Yang F, Tang Q, Zhong X, et al. Surface decoration by Spirulina polysaccharide enhances the cellular uptake and anticancer efficacy of selenium nanoparticles. *Int J Nanomedicine*. 2012;7:835–844.
20. Cheung JY, Ong RC, Suen YK, et al. Polyphyllin D is a potent apoptosis inducer in drug-resistant HepG2 cells. *Cancer Lett*. 2005;217(2):203–211.
21. Chen T, Wong YS. Selenocystine induces reactive oxygen species-mediated apoptosis in human cancer cells. *Biomed Pharmacother*. 2009;63(2):105–113.
22. Chen T, Zheng W, Wong YS, Yang F. Mitochondria-mediated apoptosis in human breast carcinoma MCF-7 cells induced by a novel selenadiazole derivative. *Biomed Pharmacother*. 2008;62(2):77–84.
23. Mu H, Wang X, Lin PH, Yao Q, Chen C. Chlorotyrosine promotes human aortic smooth muscle cell migration through increasing superoxide anion production and ERK1/2 activation. *Atherosclerosis*. 2008;201(1):67–75.
24. Petersen H, Fechner PM, Martin AL, et al. Polyethylenimine-graft-poly(ethylene glycol) copolymers: influence of copolymer block structure on DNA complexation and biological activities as gene delivery system. *Bioconjug Chem*. 2002;13(4):845–854.
25. Yeo JK, Cha SD, Cho CH, et al. Se-methylselenocysteine induces apoptosis through caspase activation and Bax cleavage mediated by calpain in SKOV-3 ovarian cancer cells. *Cancer Lett*. 2002;182:83–92.
26. Chen T, Wong YS. Selenocystine induces caspase-independent apoptosis in MCF-7 human breast carcinoma cells with involvement of p53 phosphorylation and reactive oxygen species generation. *Int J Biochem Cell Biol*. 2009;41:666–676.
27. Tian Q, Zhang CN, Wang XH, et al. Glycyrrhetinic acid-modified chitosan/poly(ethylene glycol) nanoparticles for liver-targeted delivery. *Biomaterials*. 2010;31(17):4748–4756.
28. Evan G, Littlewood T. A matter of life and cell death. *Science*. 1998;281(5381):1317–1322.
29. Kim R. Recent advances in understanding the cell death pathways activated by anticancer therapy. *Cancer*. 2005;103(8):1551–1560.
30. van Gurp M, Festjens N, van Loo G, Saelens X, Vandenabeele P. Mitochondrial intermembrane proteins in cell death. *Biochem Biophys Res Commun*. 2003;304(3):487–497.
31. Zamzami N, Marchetti P, Castedo M, et al. Sequential reduction of mitochondrial transmembrane potential and generation of reactive oxygen species in early programmed cell death. *J Exp Med*. 1995;182(2):367–377.
32. Peled-Kamar M, Lotem J, Okon E, Sachs L, Groner Y. Thymic abnormalities and enhanced apoptosis of thymocytes and bone marrow cells in transgenic mice overexpressing Cu/Zn-superoxide dismutase: implications for Down syndrome. *EMBO J*. 1995;14(20):4985–4993.
33. Peng D, Zhang J, Liu Q, Taylor EW. Size effect of elemental selenium nanoparticles (Nano-Se) at supranutritional levels on selenium accumulation and glutathione S-transferase activity. *J Inorg Biochem*. 2007;101(10):1457–1463.
34. Xiao L, Xiong X, Sun X, et al. Role of cellular uptake in the reversal of multidrug resistance by PEG-b-PLA polymeric micelles. *Biomaterials*. 2011;32(22):5148–5157.
35. Herrmann S, Winter G, Mohl S, Siepmann F, Siepmann J. Mechanisms controlling protein release from lipidic implants: effects of PEG addition. *J Control Release*. 2007;118(2):161–168.
36. Prego C, Torres D, Fernandez-Megia E, Novoa-Carballal R, Quinoa E, Alonso MJ. Chitosan-PEG nanocapsules as new carriers for oral peptide delivery. Effect of chitosan pegylation degree. *J Control Release*. 2006;111(3):299–308.
37. Vila A, Sanchez A, Tobio M, Calvo P, Alonso MJ. Design of biodegradable particles for protein delivery. *J Control Release*. 2002;78(1–3):15–24.